Available online at www.sciencedirect.com

ScienceDirect

Journal of the European Ceramic Society 35 (2015) 1123–1127

www.elsevier.com/locate/jeurceramsoc

Short communication

Design of interfaces for optimal mechanical properties in Al_2O_3/Mo laminated composites

Junjie Song [a,b], Yongsheng Zhang [a,*], Hengzhong Fan [a,b], Tianchang Hu [a], Litian Hu [a,*], Jianmin Qu [c]

[a] *Lanzhou Institute of Chemical Physics, Chinese Academy of Sciences, Lanzhou 730000, China*
[b] *University of Chinese Academy of Sciences, Beijing 100049, China*
[c] *Northwestern University, Evanston, IL 60201, USA*

Received 16 May 2014; received in revised form 28 August 2014; accepted 9 September 2014
Available online 22 October 2014

Abstract

High-performance Al_2O_3/Mo laminated composites are potential candidates for space applications because of their excellent self-lubricating and mechanical performance. This study aims at revealing the mechanisms of how interfacial morphology affects the mechanical properties of Al_2O_3/Mo laminated composites. Four types of micro-textures of different densities were produced by solid-state pulse Nd:YAG laser on the surface of a Al_2O_3 green body. Al_2O_3/Mo laminated composites with different interfacial morphologies were prepared by laser-texturing and hot-pressing. It is found that the self-locking function of a regular serrated interface improves the interfacial bonding strength and controls the residual stress of materials, thus realizing the optimization of materials. The toughness, work of fracture and strength of the materials could reach 8.0 MPa $m^{1/2}$, 1179 J m^{-2} and 293 MPa, which were 2.1 times, 6.6 times and 1.2 times higher than those of monolithic Al_2O_3 ceramics, respectively.

Keywords: Ceramic matrix composites (CMC); Layered structures; Interface structure; Mechanical properties

1. Introduction

Lamination is one of the new strategies being used to enhance the mechanical properties of ceramics.[1,2] During the past decade, inspiration from bionic multilayer structures like shells, which are mounts of layered ceramic composites, has been studied.[3–5] Combining the bionic design of ceramic materials and self-lubricating ceramic–matrix composites with excellent lubricating property is a promising way to achieve the integration of mechanical and tribological properties.[6–8] According to a previous study, Al_2O_3/Mo composites with a laminated structure have excellent self-lubricating and mechanical properties.[8] These multilayer materials consist of a weak interfacial layer of Mo, which results in high fracture toughness and low friction coefficient. The bending strength of the material can reach properties similar to those of general monolithic Al_2O_3 ceramics, and the friction coefficient of the material can be as low as 0.34 at 800 °C, which is more than 60% lower than that of the monolithic Al_2O_3 ceramics. These excellent tribological and mechanical properties enable many potential high-technology applications as structural materials. However, the in-depth and systematic studies on these materials are few, especially on their optimal design of the interface, which is the key to the practical application of the materials.

For ceramic–metal laminated composites, interfacial characteristics may have an important effect on their mechanical properties.[9–13] Any modification of the interface will be a determining factor in the strength of the interfacial bond and will eventually affect the toughness, strength, and fracture behavior of laminated composites.[14–18] Moreover, the crack path and interfacial fracture resistance depend on the interfacial bonding strength of laminated composites.[19–21] Therefore, adjusting the interface characteristics is an effective method to achieve property control. The aim of this study is to analyze the interfacial morphology influence on the mechanical properties of Al_2O_3/Mo laminated composites and to guide the optimization

* Corresponding author. Tel.: +86 931 4968833; fax: +86 931 8277088.
E-mail address: zhysh@licp.cas.cn (Y. Zhang).

http://dx.doi.org/10.1016/j.jeurceramsoc.2014.09.023
0955-2219/

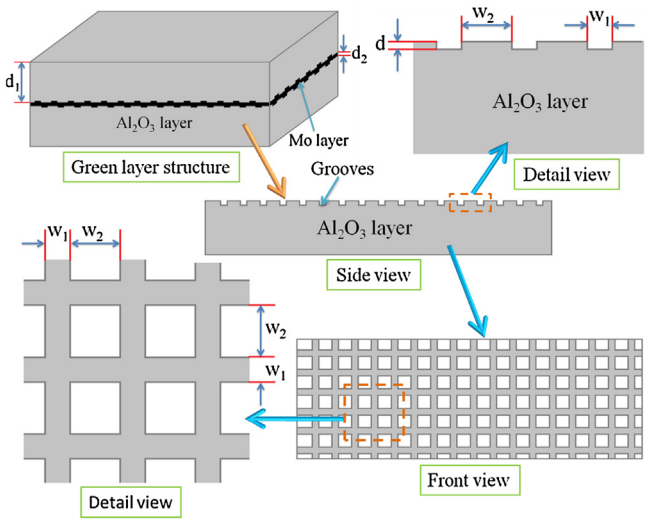

Fig. 1. The schematic diagram of the Al_2O_3/Mo laminated composites: the green body structure, side view, front view and detailed view of the textured Al_2O_3 Layer.

design of Al_2O_3/Mo multilayer composites through interfacial control. The followings are the main objectives of this research: (1) fabricate Al_2O_3/Mo laminated composites with different controllable textured interfaces (interfacial morphology), (2) analyze the relationship between the interfacial morphology and mechanical property of materials, and (3) discuss and put forward the mechanism of how interfacial morphology affects the mechanical properties of Al_2O_3/Mo laminated composites.

2. Experimental procedure

Fig. 1 and Table 1 illustrate the schematic and the design concept of Al_2O_3/Mo laminated composites. The thickness of the Al_2O_3 layer and the Mo layer are d_1 and d_2, respectively. The groove width of the textured layer is W_1, groove interval is W_2, and the depth d of the grooves is about 60 μm. The geometrical parameters of the grooves of the samples are given in Table 1, where A_d is the area density of the grooves at the interface. We obtained the A_d from the formula $A_d = 1 - {W_2}^2/(W_1 + W_2)^2$.

Commercially available Mo (≤4 μm) and micro-/nano-sized Al_2O_3 powders (33–1100 nm)[22] were used in this study. The steps to manufacture the materials are as follows: (1) prepare the untextured or textured Al_2O_3 layers, (2) alternately stack the Al_2O_3 layers and Mo powders in graphite mold layer by layer, and (3) hot-press the graphite mold. The monolithic Al_2O_3 samples and the Al_2O_3 layer of the laminated samples were prepared by placing the Al_2O_3 powders into a steel mold with a definite weight and then dry-pressing them at 180 MPa for 5 min. The interfacial texture was prepared on the surface of the Al_2O_3 layer for the laminated samples using a commercial pulse Nd:YAG laser. The laser had a wavelength of 1064 nm and mean power of 10 W. A pulsing frequency of 15 kHz, scanning speed of 5 mm s^{-1}, and an overlapping rate of 94% for laser spot were used to produce micro-grooves on the surface of the Al_2O_3 layer. After laser ablation, the textured Al_2O_3 layers with a delicate surface morphology were obtained using a hair drier to remove the scrap around the grooves. The green bodies of monolithic and laminated samples were sintered by hot-pressing at 1550 °C and 25 MPa for 90 min in an argon atmosphere.

Macroscopic features and microstructures of the Al_2O_3/Mo laminated composites were observed under optical microscopy, Micro XAM 3D profilometer and JSM-5600LV scanning electron microscopy (SEM), respectively. The structures and chemical compositions of the sintered composites were determined by X-ray diffraction (XRD) and energy dispersive spectrometer (EDS). The rectangular beams for mechanical tests were conducted on a universal testing machine (DY35) at room temperature. The dimensions of the rectangular beams for the toughness and bending strength tests were 25 mm × 1.9 mm × 3.7 mm and 25 mm × 4 mm × 3.7 mm, respectively. Bending strength (σ) was determined by a three-point bending test with a span of 20 mm and a cross-head rate of 0.5 mm min^{-1}.[7,23] The toughness (K_{app}) was determined with the same three-point bending test fixture with a span of $L = 16$ mm and a cross-head speed of 0.05 mm min^{-1} using a single-edge notched beam (SENB) specimen with a ~1.75 mm deep and ~0.20 mm thick notch (inserted at the upper right corner of Fig. 3b). Note that the middle Mo layer was retained when sawing the notch and each notch tip was sharpened (radius <20 μm) by a razor blade prior to the test. There is a small distance between notch-tip and Mo layer, which is mainly to avoid destroying the integrity of Mo layer, and ensure the initial crack extension will take place firstly at Al_2O_3 part between notch-tip and Mo layer. The toughness was obtained from the equation given by Zhang.[23] Work of fracture was calculated from the formula $\gamma_{WOF} = \int Pd\delta/A$ ($\int Pd\delta$ is the total energy of the applied load and A is the projection area of fractural surface), and the quantitative value of $\int Pd\delta$ was achieved by the load–displacement curve in toughness. The double-shearing method (inserted at the lower left corner of Fig. 3a) was used to determine the interfacial bonding strength, with a span length of 5 mm and a cross-head rate of 0.05 mm min^{-1}. Each specimen for the double-shearing test was prepared by the same preparing method of laminated materials (three Al_2O_3 layers and two Mo layers) with dimension of 12 mm × 5 mm × 8 mm. Two notches about 2 mm deep were sawed by a 0.20 mm-thick diamond disk in the upper and lower ends of the test specimen parallel to the Mo layer, which is to ensure that the initial crack could be initiated at the interface. And the interfacial bonding strength was calculated from the formula $\tau = P_{MAX}/2S$ (P_{MAX} is the maximum load in double shearing test and S is the actual interfacial area).

3. Results and discussion

Fig. 2 shows the interfacial and profile microstructures of the Al_2O_3/Mo laminated composites. As shown in Fig. 2a and b, the grooves on the surface of the textured Al_2O_3 layers are clear and uniform, and the plateau around the grooves remains smooth. The groove depth and width are 60 μm and 200 μm, respectively, for all the grooves of the textured Al_2O_3 layers.

The laminated structure with a relatively straight interface can be observed without clear delamination and pores after

Table 1
The geometry characteristics and mechanical properties of samples.

Sample	Geometry characteristics							Mechanical properties			
	W_1 (mm)	W_2 (mm)	A_d (%)	d_1 (mm)	d_2 (mm)	Layer number		τ (MPa)	K_{app} (MPa m$^{1/2}$)	γ_{WOF} (J m^{-2})	σ (MPa)
						Al_2O_3	Mo				
A	0.2	1.6	21.0	1845	42	2	1	18.1 ± 0.8	6.1 ± 0.8	264	258
B	0.2	1.2	26.5	1845	42	2	1	21.8 ± 0.5	7.9 ± 0.2	339	310
C	0.2	0.8	36.0	1845	42	2	1	26.9 ± 0.6	6.7 ± 0.5	274	297
D	0.2	0.4	55.6	1845	42	2	1	34.9 ± 1.4	5.3 ± 0.3	196	269
E	Untextured interface			1845	42	2	1	Interfacial failure occurred in the machining process			
F	–	–	–	3354	0	1	0	–	3.9 ± 0.1	179	251
G	0.2	1.2	26.5	912	42	4	3	21.8 ± 0.5	8.0 ± 0.3	1179	293

sintering (Fig. 2c). Metal Mo and Al_2O_3 have compact crystallized structures and no obvious flaws in them. Furthermore, the boundary between the Al_2O_3 layer and the Mo layer is sharp. The compositions of the specimen are α-Al_2O_3 and Mo, and the element contains Al, O, and Mo, as indicated by the XRD and EDS test results. Moreover, the serrated interfacial morphology remains clearly visible, and this interfacial characteristic not only increase the contact area between the two layers but also use the mechanical interlock effectively.

Rupture of Mo layer and delamination are the two main interface failure modes in double-shearing (Fig. 3a). After the crack is initiated, delamination occurs firstly at the smooth interface because of the relatively weak interfacial bonding strength. As the crack propagates along the interface, the crack tip is resisted by the raised area of the Mo layer, resulting in the occurrence of the rupture of Mo layer. The higher the area density of the grooves, the stronger the interfacial bonding (Table 1). Therefore, the interfacial bonding strength can be easily adjusted by this interface morphology design.

According to the above discussion, we assume that the contribution to the interfacial bonding strength of the rupture of Mo layer and delamination is B_r and B_d for every unit area, respectively. All B_d are the same for the Al_2O_3/Mo laminated composites because of the delamination mode in double-shearing test, as illustrated in Fig. 3a. Therefore, the interfacial bonding strength can be expressed by the following formula:

$$\tau = A_d \times B_r + B_d. \quad (1)$$

The approximate values of B_r and B_d achieved by substituting A_d and τ into formula (1) are as follows:

$$B_r = 46.8 \text{ MPa} \quad B_d = 9.4 \text{ MPa} \quad (2)$$

Consequently, for this interface design strategy, the interfacial bonding strength can be calculated by the following:

$$\tau = 46.8 \times A_d + 9.4. \quad (3)$$

Based on these analyzes, it also can be seen that the contribution to the interfacial bonding strength of the rupture of Mo layer is more than the delamination's. Consequently, the interfacial bonding strength could not resist the driving force for delamination of the layers without any texturing on the interface due to much residual stress being developed between two dissimilar materials on cooling. This residual stress is the reason interfacial failure occurred in Sample E, in the process of mechanical cutting. That reinforces the importance of this interfacial design which not only could adjust the mechanical properties of the laminated composites also ensure their practical functionality. In addition, to obtain the maximum toughening effect, the interfacial bonding strength must be moderate and suitable.[14] A reasonable interfacial texture exists for outstanding mechanical properties. As shown in Table 1, the toughness, fracture strength and work of fracture of the material can reach 7.9 MPa m$^{1/2}$, 310 MPa and 339 J m^{-2} when the area density of the interfacial texture is 26.5%, which is approximately 102.6%, 23.4% and 88.9% higher, respectively, than those of monolithic Al_2O_3 ceramics (sample F). Moreover, with a further increase

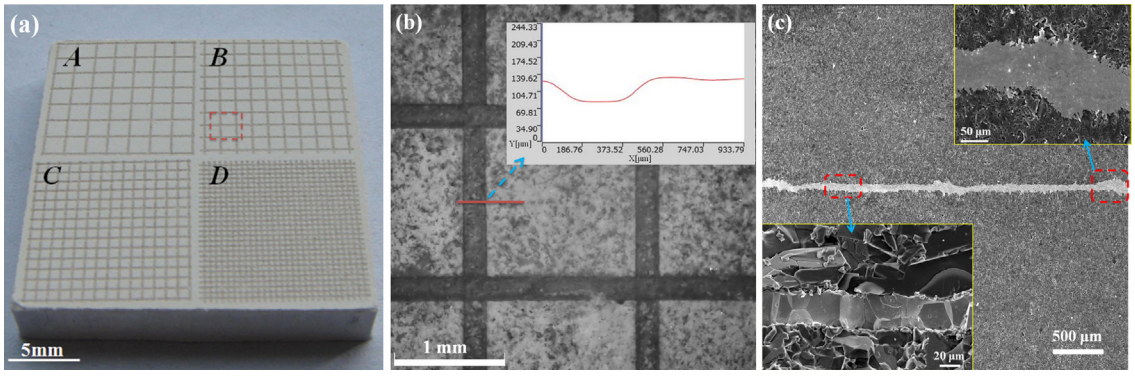

Fig. 2. The interfacial and profile microstructures of the Al_2O_3/Mo laminated composites: (a) macroscopic features of four kinds of textured Al_2O_3 layers, (b) microstructure of textured interface, (c) profile microstructure of sintering specimens.

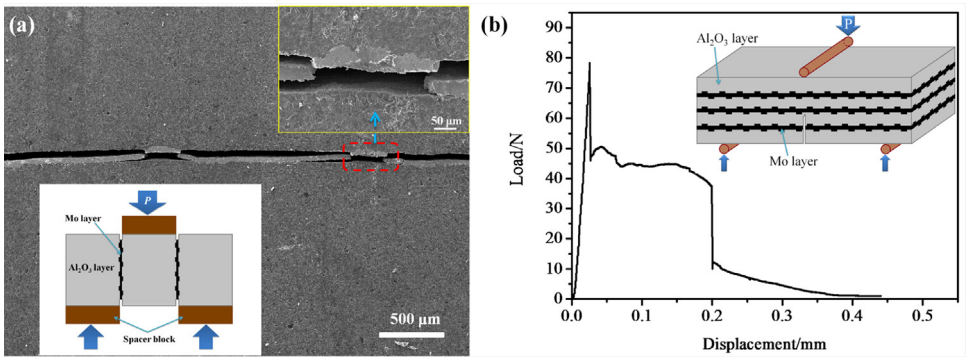

Fig. 3. SEM images of the crack-path in double-shearing (a) and load–displacement curves of the Al_2O_3/Mo laminated composites in fracture toughness (b, sample G).

in layer-number of Mo, this effect becomes more apparent. The work of fracture of material can reach 1179 J m^{-2} when the layer-number of Mo is 3 (sample G), and the load–displacement curves shows a typical non-catastrophic characteristic (Fig. 3b).

Therefore, the performance of the Al_2O_3/Mo multilayer composites can be improved significantly by introducing a regular serrated interface between the layers. The area density of the grooves plays a key role in the optimization of material properties. This is mainly for two reasons. First of all, when the crack propagates into the interfacial layer, delamination initially occurs at the smooth interface because of relatively weak interfacial bonding strength. As the crack propagates along the interface, the crack tip is dulled and resisted by the raised area of the Mo layer, resulting in the occurrence of the rupture of Mo layer (Fig. 4b). This dissipation mechanism is good for the toughness and work of fracture. Whereas if the value of W_2 is too low, the initial crack will propagates through Mo layer without any deflection at interface and resistance from the raised area of the Mo layer (Fig. 4a). However, more plastic deformation occurs in laminated composites with a higher W_2 value than a lower W_2 value (due to lower constraint among layers). [15] The more plastic deformation occurs, the more beneficial it is to the improvement of the toughness. If the value of W_2 is extremely high, the crack tip will kink into the next layer immediately after a small defection at the interface, before it be dulled by the raised area of the Mo layer (Fig. 4c). Therefore, the value of W_2 must be moderate for getting the maximum toughening effect.

Second, residual stress, which is caused by the mismatch of the thermal expansion of ceramic and metal, also contributes to incremental toughness.[24] The mismatch of the thermal expansion coefficient of Al_2O_3 (8.5×10^{-6} K^{-1}) and Mo (5.2×10^{-6} K^{-1}) results in the generation of residual tensile stress and residual compressive stress in the Al_2O_3 layer and Mo layer, respectively. When tested in SENB, the compressive layer would hinder the crack propagation, increasing materials toughness and work of fracture.[25] Consequently, the laminated composites have higher apparent toughness compared to the monolithic Al_2O_3 ceramics without crack-growth resistance. Moreover, the level of residual stress controls the apparent fracture toughness.[26] Fortunately, the residual stress between the layers of Al_2O_3/Mo composites can be adjusted easily by this interfacial design. This is mainly because the mechanical interlock among layers can effectively control the creep of layers. And the creep is conductive to the release of residual stress on cooling. Therefore, the value W_2 is excessively high, resulting in lower residual compressive stress in internal layer due to lower creep constraint.[25] Lower residual compressive stress results in lower apparent toughness. And the residual stress will remain unchanged with the increase of W_2 value, when there exist enough creep constraint to resist the creep among layers. Moreover, the residual stresses have an effective effect on the fracture strength of Al_2O_3/Mo laminated composites. The thin compressive Mo layers within Al_2O_3/Mo laminated composites can arrest large cracks, produce a threshold strength, and act as

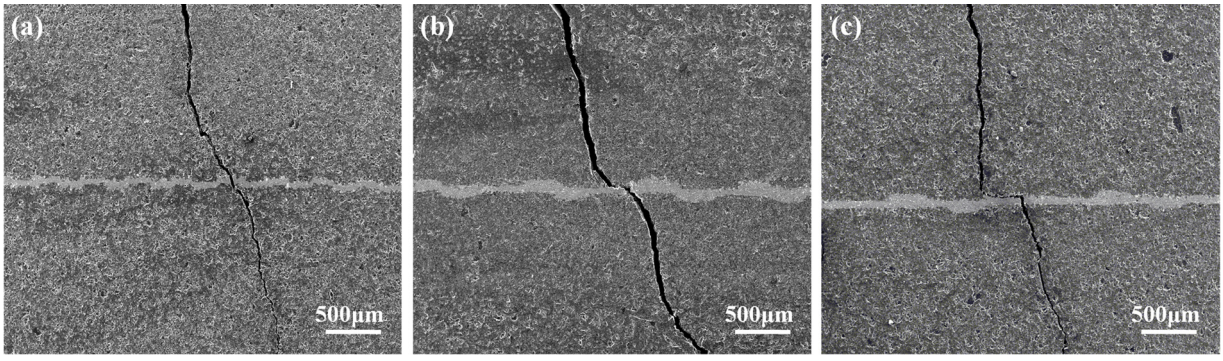

Fig. 4. The crack-path of Al_2O_3/Mo laminated composites in a three-point bending test: (a) sample D, (b) sample B, (c) sample A.

a barrier to crack extension.[25,27,28] And the higher compression is, the higher failure stress will be.[29] That is why the Al_2O_3/Mo laminated composites have higher bending load compared to the monolithic Al_2O_3 ceramics without crack-growth resistance. Taking all those affecting factors into account, if want to get the optimum performance, the value of W_2 must be moderate. When the value W_2 is approximately 1.2 mm, which is more beneficial to the improvement of fracture toughness.

4. Conclusions

In summary, this work demonstrates that the method is simple and effective in achieving the interfacial control of Al_2O_3/Mo laminated composites by laser texturing. The interfacial design methodology presented in this paper not only ensures the practical functionality of Al_2O_3/Mo laminated composites but also improves the mechanical properties of composites. The combined actions of the interfacial bonding strength, interfacial morphology, and residual stress between the layers influence the apparent toughness of the materials. Our experimental studies show that the toughness and work of fracture of the material can reach 8.0 MPa $m^{1/2}$ and 1179 J m^{-2} when the area density of the interfacial texture is 26.5%, which are approximately 2.1 times and 6.6 times higher than those of monolithic Al_2O_3 ceramics, respectively.

Acknowledgements

The authors acknowledge financial support from the National Natural Science Foundation of China (51175493), the National Basic Research Program of China (973 Program, 2011CB706603) and the Program of the Light of the Chinese Academy of Sciences in China's Western Region (2010).

Appendix A. Supplementary data

Supplementary data associated with this article can be found, in the online version, at http://dx.doi.org/10.1016/j.jeurceramsoc.2014.09.023.

References

1. Clegg WJ, Kendall K, Alford NM, Button TW, Birchall JD. A simple way to make tough ceramics. *Nature* 1990;**347**:455–7.
2. Huang Y, Wang CA. *Multiphase composite ceramics with high performance*. 1st ed. Beijing, China: Tsinghua University Press; 2008.
3. Wang CA, Huang Y, Zan Q, Guo H, Cai S. Biomimetic structure design-a possible approach to change the brittleness of ceramics in nature. *Mater Sci Eng, C* 2000;**11**(1):9–12.
4. Mekky W, Nicholson PS. The fracture toughness of Ni/Al_2O_3 laminates by digital image correlation I: Experimental crack opening displacement and R-curves. *Eng Fract Mech* 2006;**73**(5):571–82.
5. Launey ME, Munch E, Alsem DH, Saiz E, Tomsia AP, Ritchie RO. A novel biomimetic approach to the design of high-performance ceramic–metal composites. *J R Soc Interface* 2010;**7**(46):741–53.
6. Qi Y, Zhang Y, Fang Y, Hu L. Design and preparation of high-performance alumina functional graded self-lubricated ceramic composites. *Composites, B: Eng* 2013;**47**:1–5.
7. Fang Y, Zhang Y, Song J, Fan H, Hu L. Design and fabrication of laminated-graded zirconia self-lubricating composites. *Mater Des* 2013;**49**:421–5.
8. Qi Y, Zhang Y, Hu L. High-temperature self-lubricated properties of Al_2O_3/Mo laminated composites. *Wear* 2012;**280–281**:1–4.
9. Ritchie RO, Cannon RM, Dalgleish BJ, Dauskardt RH, McNaney JM. Mechanics and mechanisms of crack growth at or near ceramic–metal interfaces: interface engineering strategies for promoting toughness. *Mater Sci Eng, A* 1993;**166**:221–35.
10. Bartolomé JF, Beltrán JI, Gutiérrez-González CF, Pechrromán C. Influence of ceramic–metal interface adhesion on crack growth resistance of ZrO_2–Nb ceramic matrix composites. *Acta Mater* 2008;**56**(14):3358–66.
11. Sherman D. The mechanical behavior of layered brazed metal/ceramic composites. *Mater Lett* 1998;**33**(5–6):255–60.
12. Biner SB. A numerical analysis of failure characteristics of ductile layers in laminated composites. *J Mater Sci* 1998;**33**(15):3953–63.
13. Dey A, Dey P, Datta S, Mukhopadhyay AK. A new model for multilayer ceramic composites. *Mater Manuf Processes* 2008;**23**:513–27.
14. Wang CA, Huang Y, Zan Q, Zou L, Cai S. Control of composition and structure in laminated silicon nitride/boron nitride composites. *J Am Ceram Soc* 2002;**85**(10):2457–61.
15. Chen Z, Mecholsky Jr JJ. Control of strength and toughness of ceramic/metal laminates using interface design. *J Mater Res* 1993;**8**(9):2362–9.
16. Chen Z, Mecholsky Jr JJ. Effect of interface design on high-temperature failure of laminated composites. *J Mater Res* 1996;**11**(8):2035–41.
17. Ranjbar-Far M, Absi J, Mariaux G, Dubois F. Simulation of the effect of material properties and interface roughness on the stress distribution in thermal barrier coatings using finite element method. *Mater Des* 2010;**31**(2):772–81.
18. Belhouari M, Bouiadjra BB, Kaddouri K, Achour T. Plasticity effect on crack growth along ceramic/metal biomaterial interface: numerical analysis. *Mech Adv Mater Struct* 2011;**18**:364–72.
19. Hwu KL, Derby B. Fracture of metal/ceramic laminates-II crack growth resistance and toughness. *Acta Mater* 1999;**47**(2):545–63.
20. Ma Q, Shaw MC, He MY, Dalgleish BJ, Clarke DR, Evans AG. Stress redistribution in ceramic/metal multilayers containing cracks. *Acta Metall Mater* 1995;**43**(6):2137–42.
21. Konopka K, Maj M, Kurzydlowskj KJ. Studies of the effect of metal particles on the fracture toughness of ceramic matrix composites. *Mater Charact* 2003;**51**(5):335–40.
22. Qi Y, Zhang Y, Hu L. Preparation and properties optimization of Al_2O_3/Al_2O_3–ZrO_2 (3Y) laminated nanocomposites. *J Mater Eng* 2013;**9**:8–12.
23. Zhang W, Telle R, Uebel J. R-curve behaviour in weak interface-toughened SiC-C laminates by discrete element modeling. *J Eur Ceram Soc* 2014;**34**(2):217–27.
24. Zuo KH, Jiang DL, Lin QL. Mechanical properties of Al_2O_3/Ni laminated composites. *Mater Lett* 2006;**60**:1265–8.
25. Bermejo R, Sanchez-Herencia AJ, Llanes L, Baudin C. High-temperature mechanical behaviour of flaw tolerant alumina–zirconia multilayered ceramics. *Acta Mater* 2007;**55**(14):4891–901.
26. Krstic Z, Krstic VD. Crack propagation and residual stress in laminated Si_3N_4/BN composite structures. *J Eur Ceram Soc* 2011;**31**(9):1841–7.
27. Rao M, Sanchez-Herencia J, Beltz G, McMeeking RM, Lange F. Laminar ceramics that exhibit a threshold strength. *Science* 1999;**286**(5437):102–5.
28. Bermejo R, Pascual J, Lube T, Danzer R. Optimal strength and toughness of Al_2O_3–ZrO_2 laminates designed with external or internal compressive layers. *J Eur Ceram Soc* 2008;**28**(8):1575–83.
29. Sglavo VM, Bertoldi M. Design and production of ceramic laminates with high mechanical reliability. *Composites, B: Eng* 2006;**37**(6):481–9.